Supplementary Materials for:

Estimating flood discharge at river bridges using the entropy theory. Insights from Computational Fluid Dynamics flow fields

Farhad Bahmanpouri[1], Tommaso Lazzarin[2], Silvia Barbetta[1], Tommaso Moramarco[1], Daniele P. Viero[2]

[1] Research Institute for Geo-Hydrological Protection, National Research Council (CNR), Perugia, 06128, Italy
[2] Department of Civil, Environmental and Architectural Engineering, University of Padova, 35131, Italy.

S1. Results for the peak-flow condition of the 2012 flood event

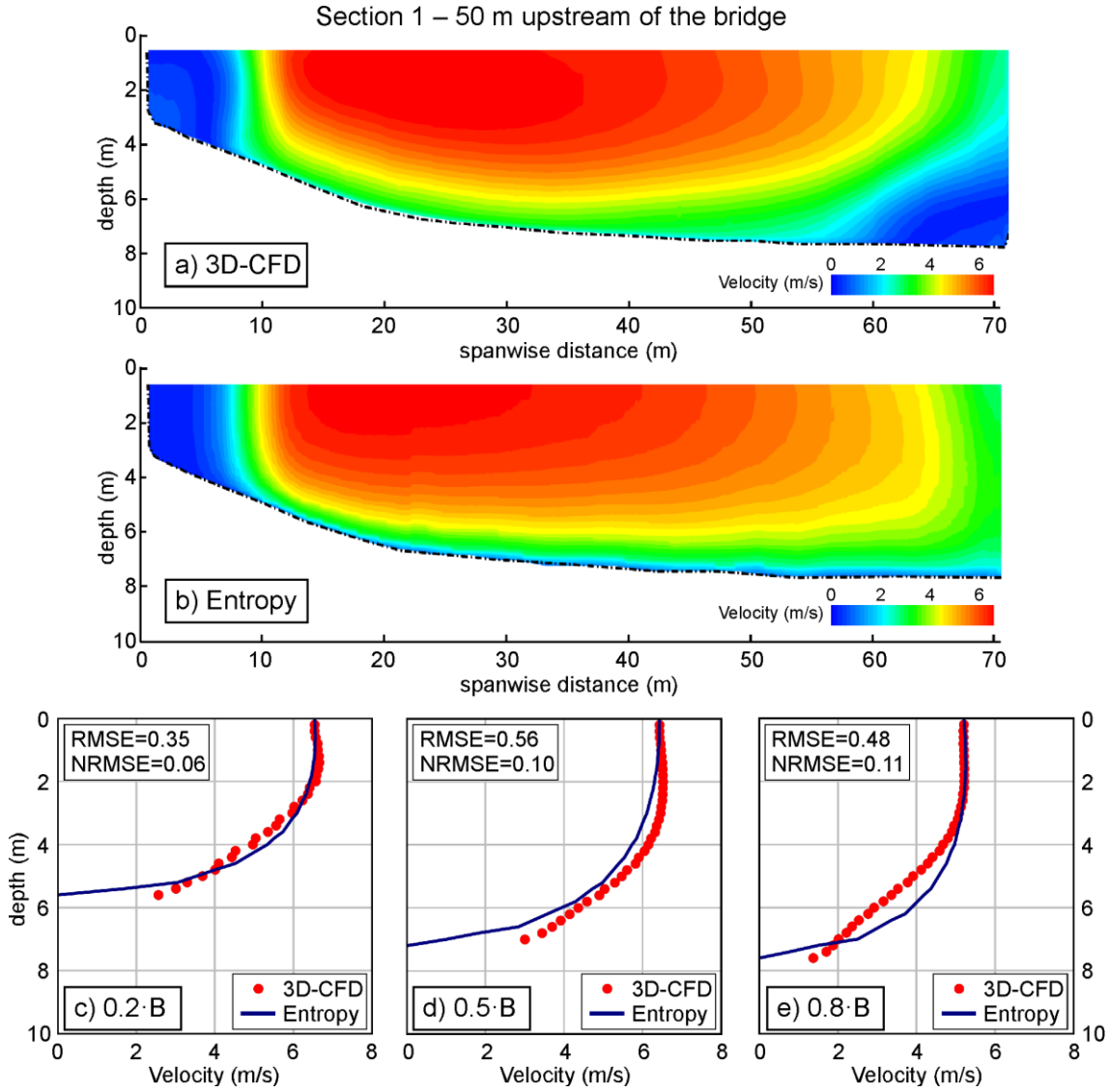

Figure S1. Flood event of 2012, cross-section 1 (50 m upstream of the bridge). Velocity distributions provided by (a) the 3D-CFD model, and (b) the entropy model forced with the river-wide distribution of the free-surface velocity. Comparison of vertical distributions of velocity at 0.2*B* (c), 0.5*B* (d), and 0.8*B* (e), where *B* is the width of the cross-section.

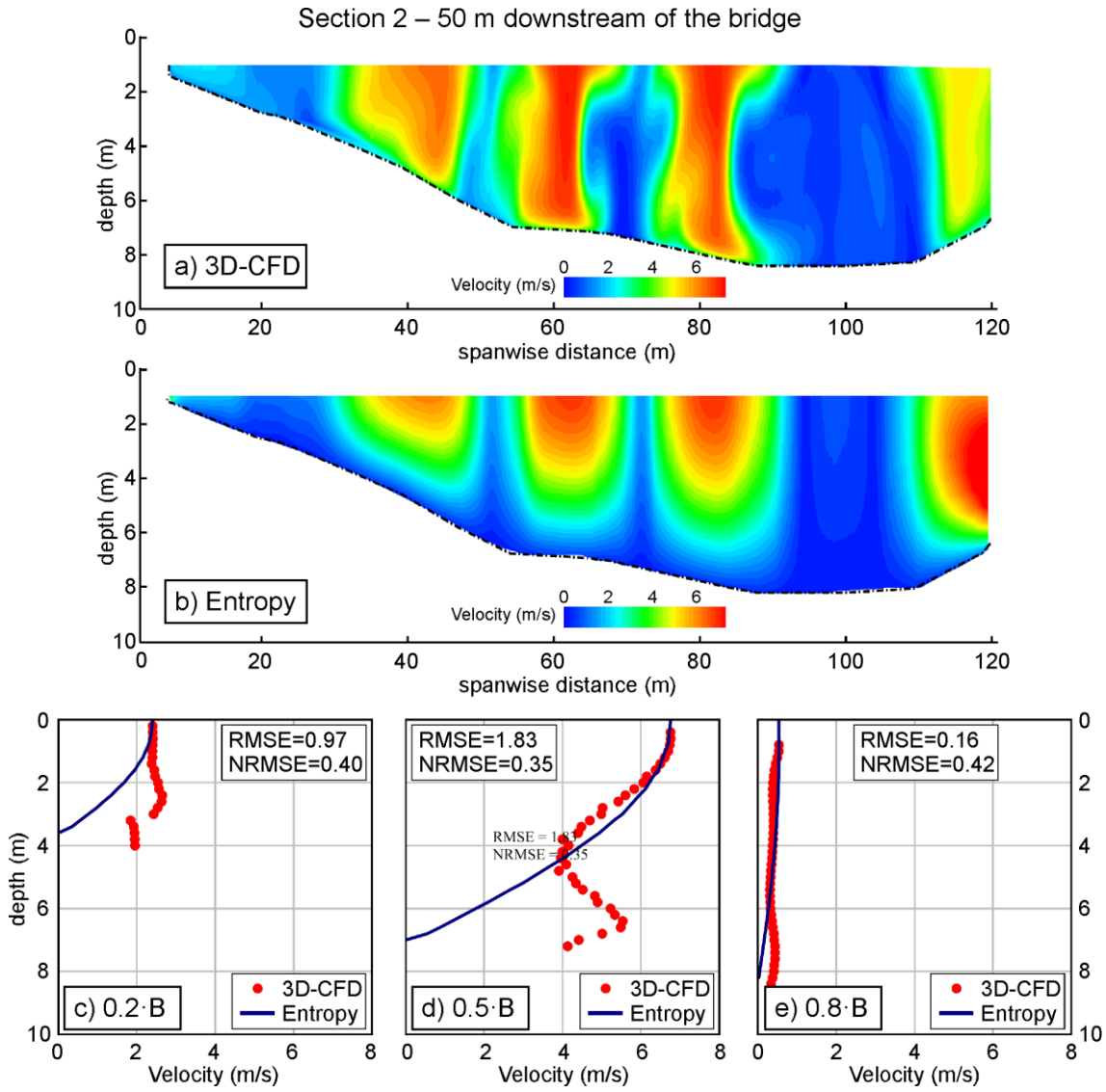

Figure S2. Flood event of 2012, cross-section 2 (50 m downstream of the bridge). Velocity distributions provided by (a) the 3D-CFD model, and (b) the entropy model forced with the river-wide distribution of the free-surface velocity. Comparison of vertical distributions of velocity at 0.2*B* (c), 0.5*B* (d), and 0.8*B* (e), where *B* is the width of the cross-section.

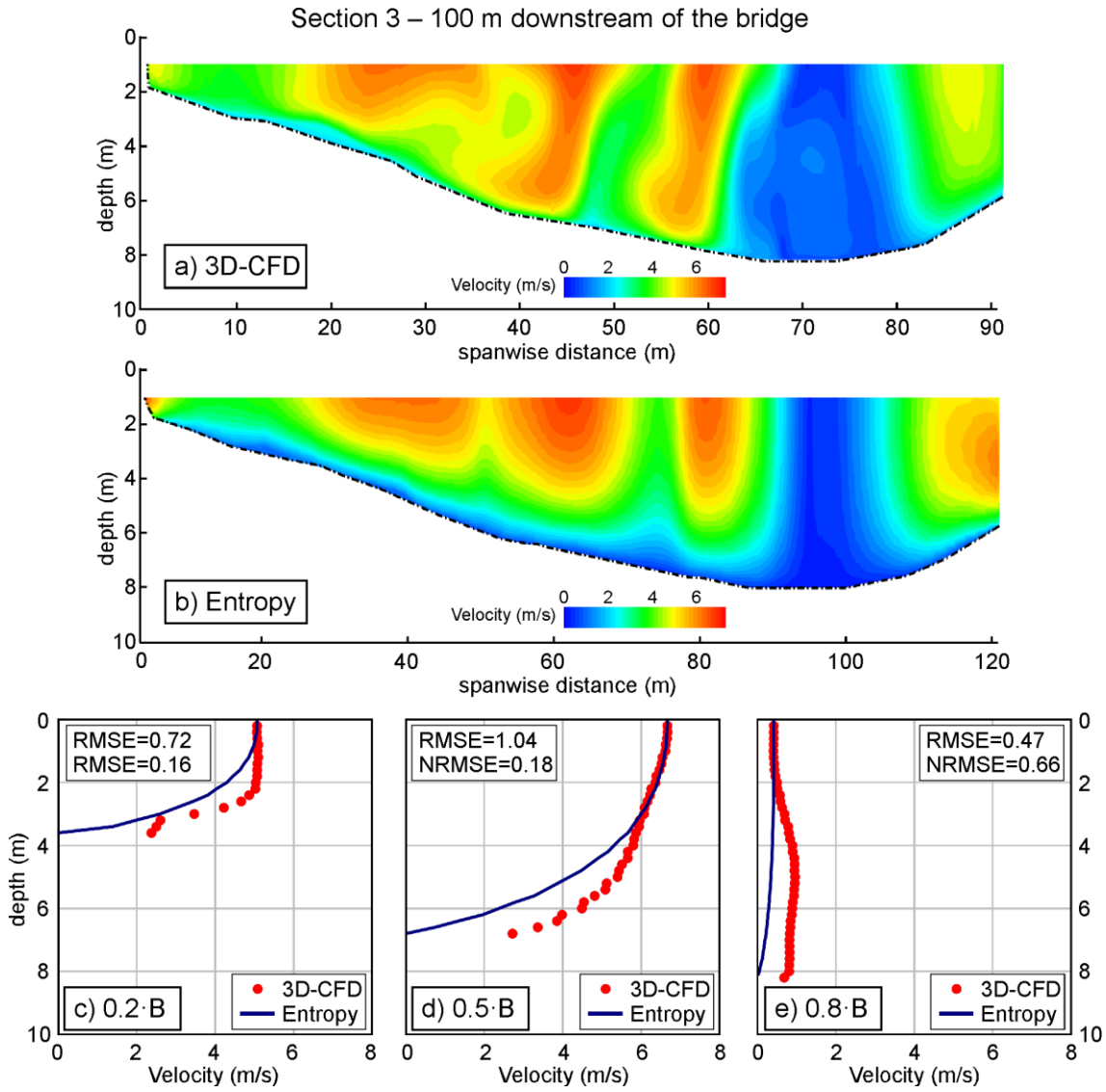

Figure S3. Flood event of 2012, cross-section 3 (100 m downstream of the bridge). Velocity distributions provided by (a) the 3D-CFD model, and (b) the entropy model forced with the river-wide distribution of the free-surface velocity. Comparison of vertical distributions of velocity at 0.2*B* (c), 0.5*B* (d), and 0.8*B* (e), where *B* is the width of the cross-section.

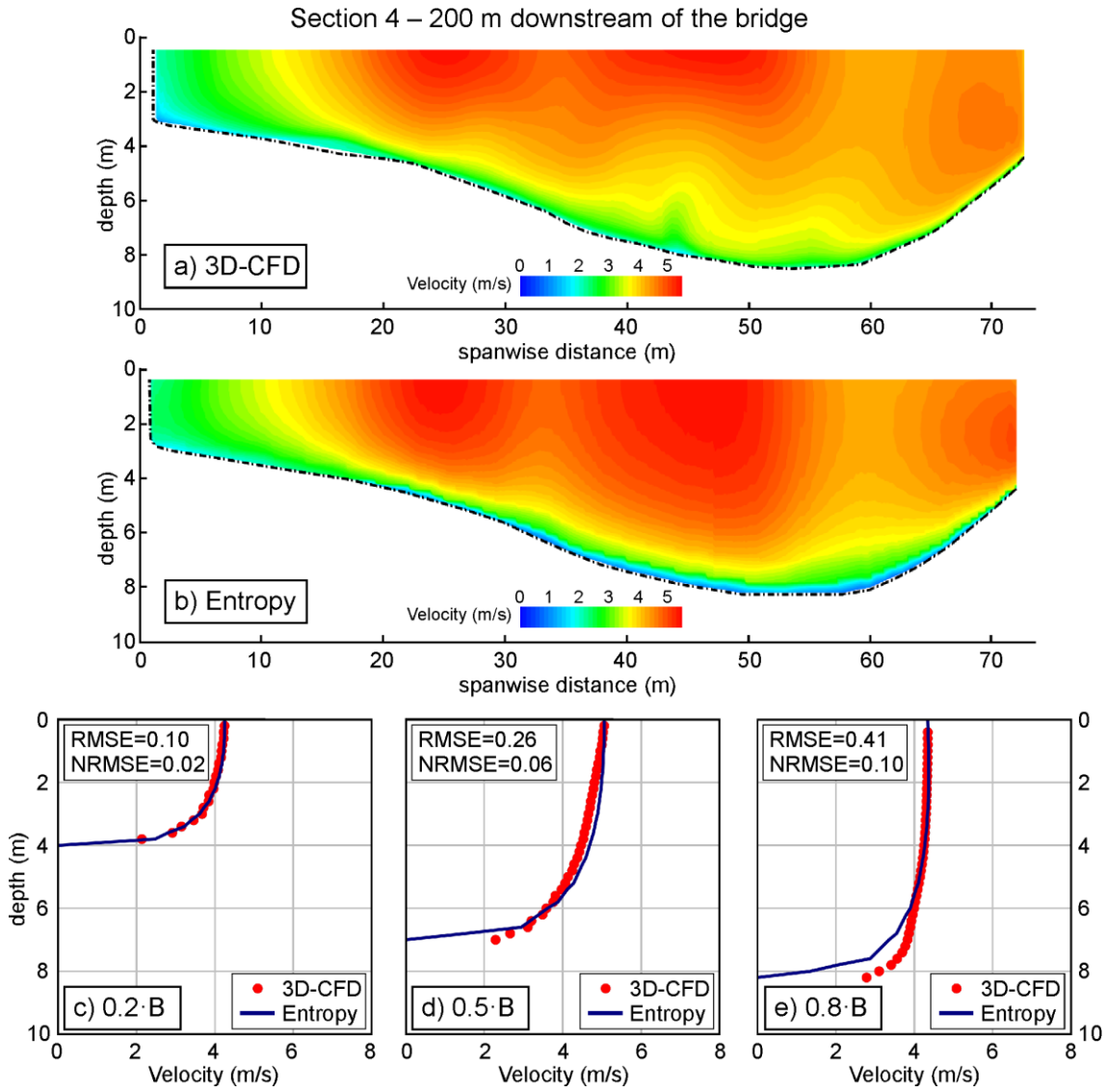

Figure S4. Flood event of 2012, cross-section 4 (200 m downstream of the bridge). Velocity distributions provided by (a) the 3D-CFD model, and (b) the entropy model forced with the river-wide distribution of the free-surface velocity. Comparison of vertical distributions of velocity at 0.2*B* (c), 0.5*B* (d), and 0.8*B* (e), where *B* is the width of the cross-section.

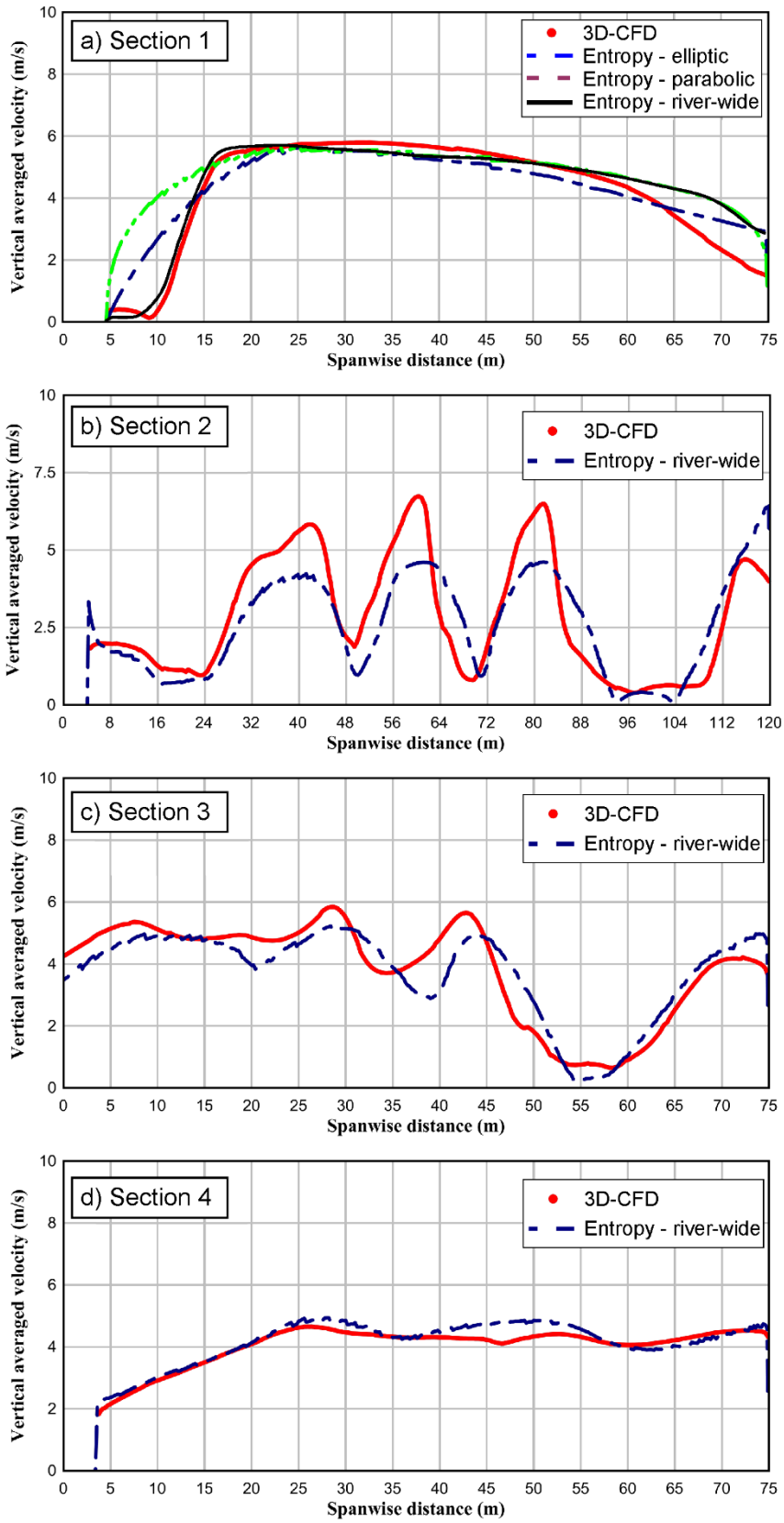

Figure S5. Flood event of 2012. Depth-averaged spanwise velocity distribution at the four cross-sections.

S2. Results for the peak-flow condition of the 2019 flood event

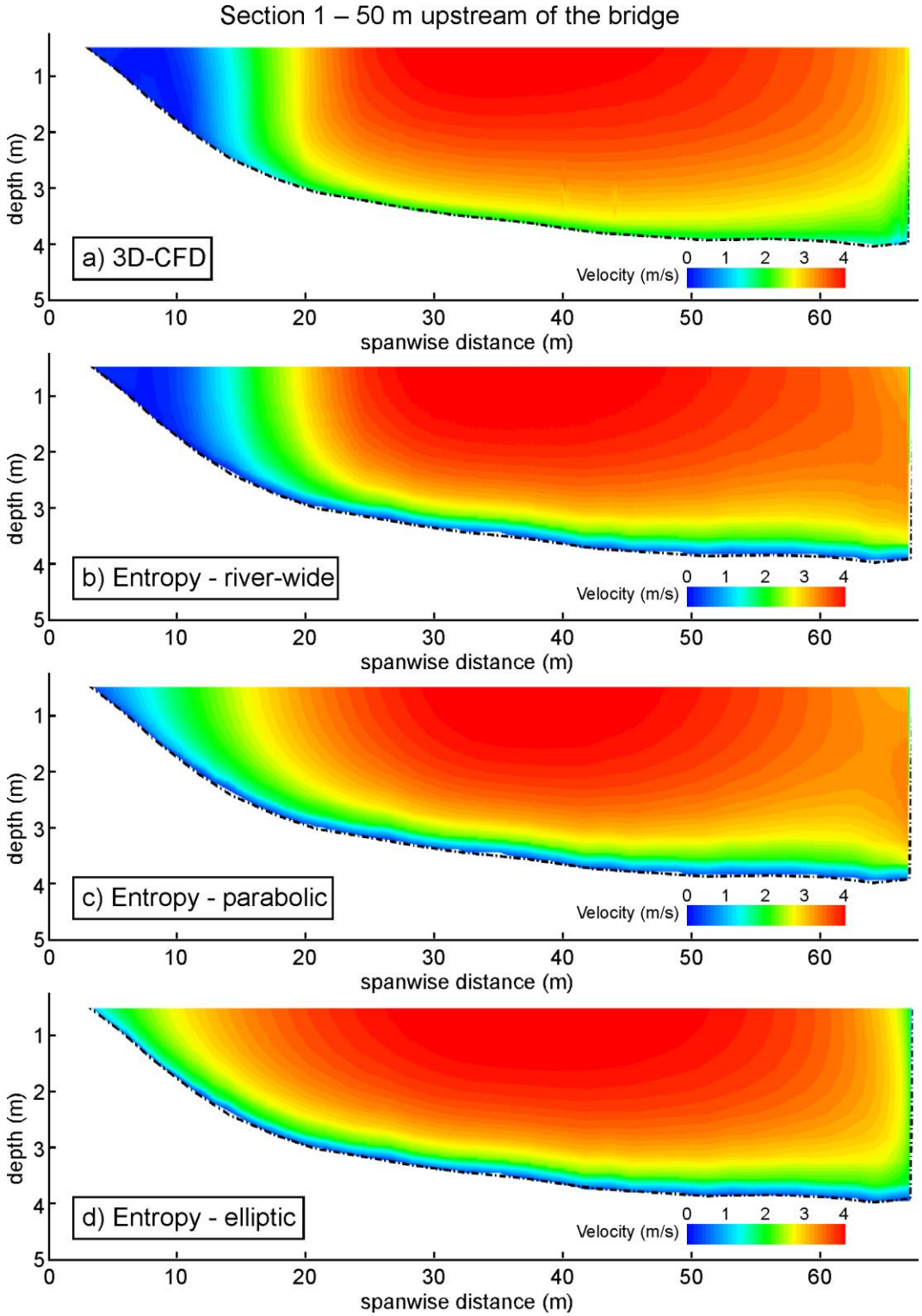

Figure S6. Flood event of 2019, cross-section 1 (50 m upstream of the bridge). Cross-sectional velocity distribution computed with the 3D-CFD model (a), and the entropy theory forced with (b) the river-wide surface velocity, (c) the parabolic, and (d) and elliptic spanwise velocity distribution.

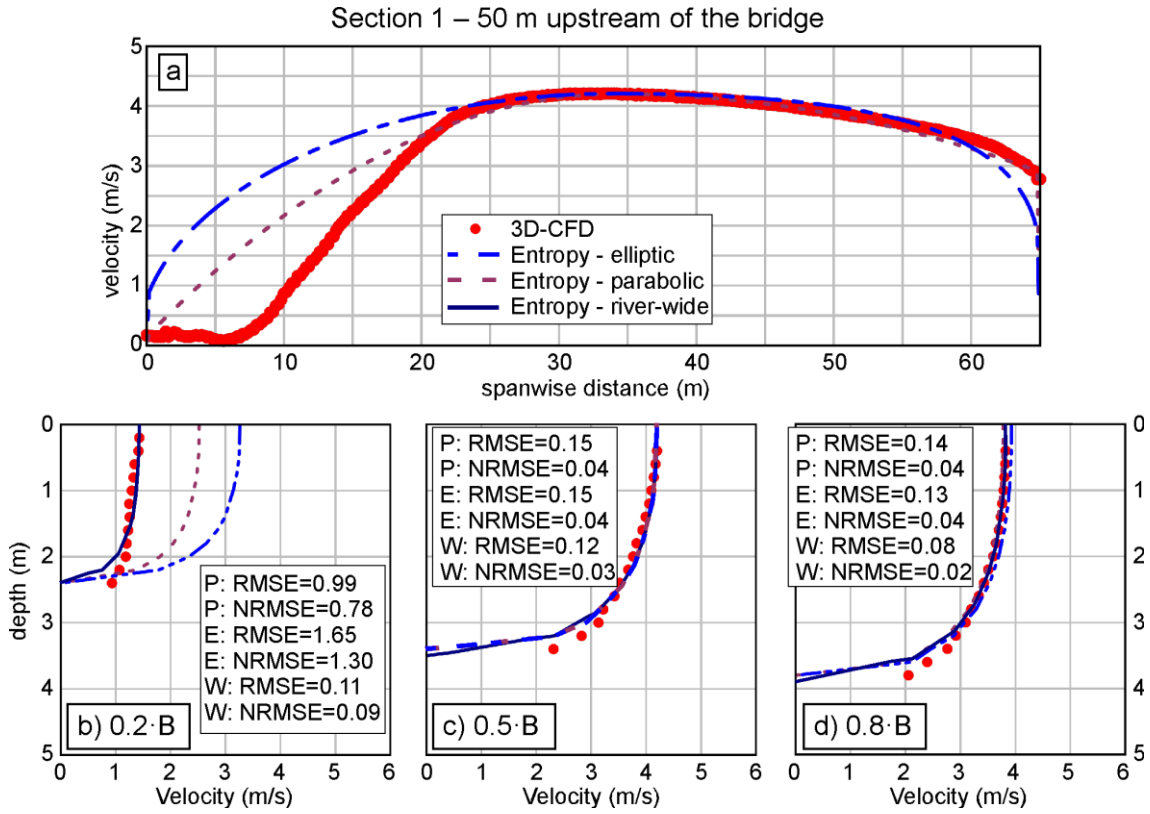

Figure S7. Flood event of 2019, cross-section 1 (50 m upstream of the bridge). Spanwise distribution of the surface velocity (a); comparison of vertical distributions of velocity at 0.2*B* (b), 0.5*B* (c), and 0.8*B* (d).

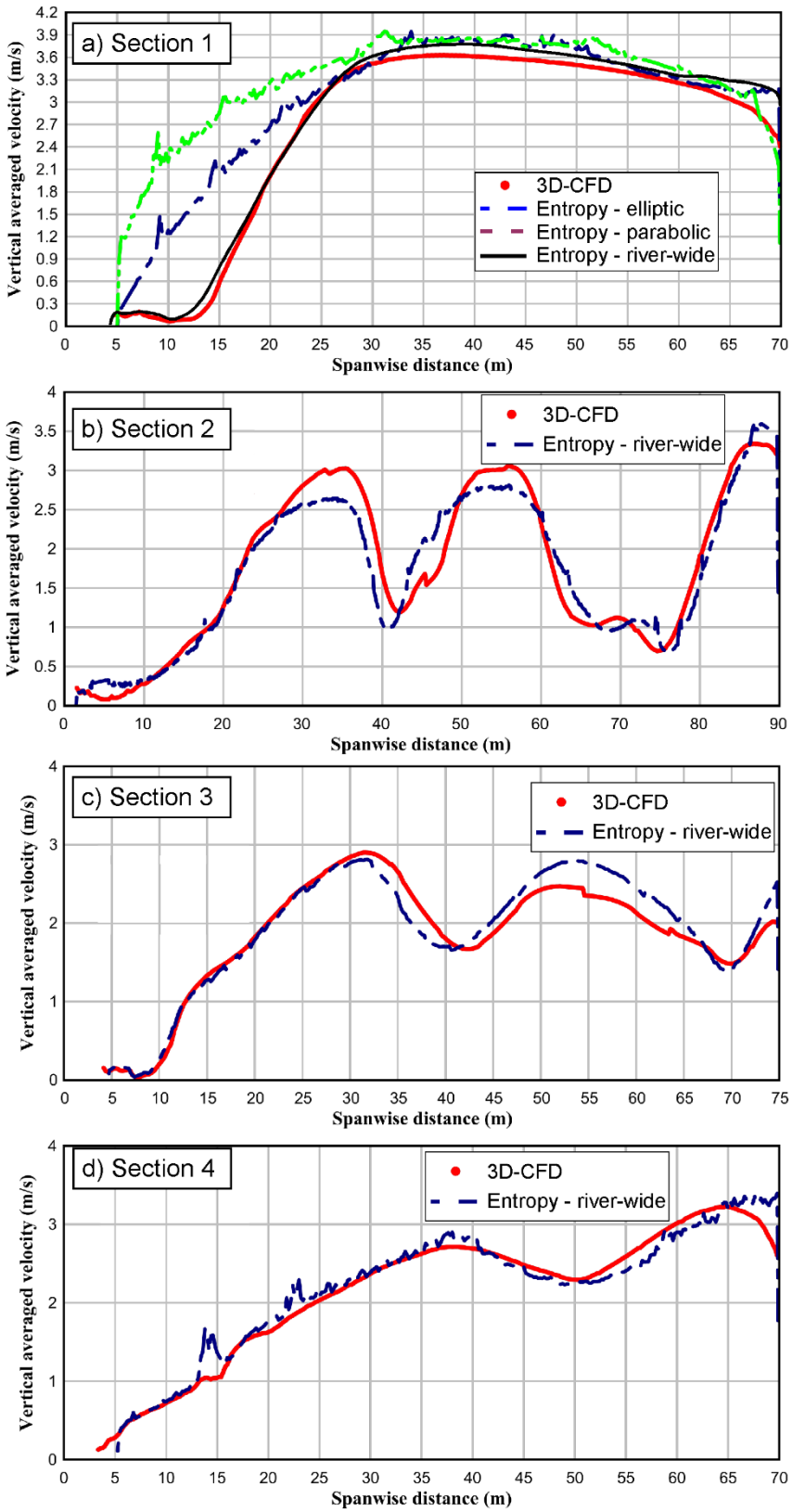

Figure S8. Flood event of 2019. Depth-averaged spanwise velocity distribution at the four cross-sections.

S3. Results for the peak-flow condition of the 2022 flood event

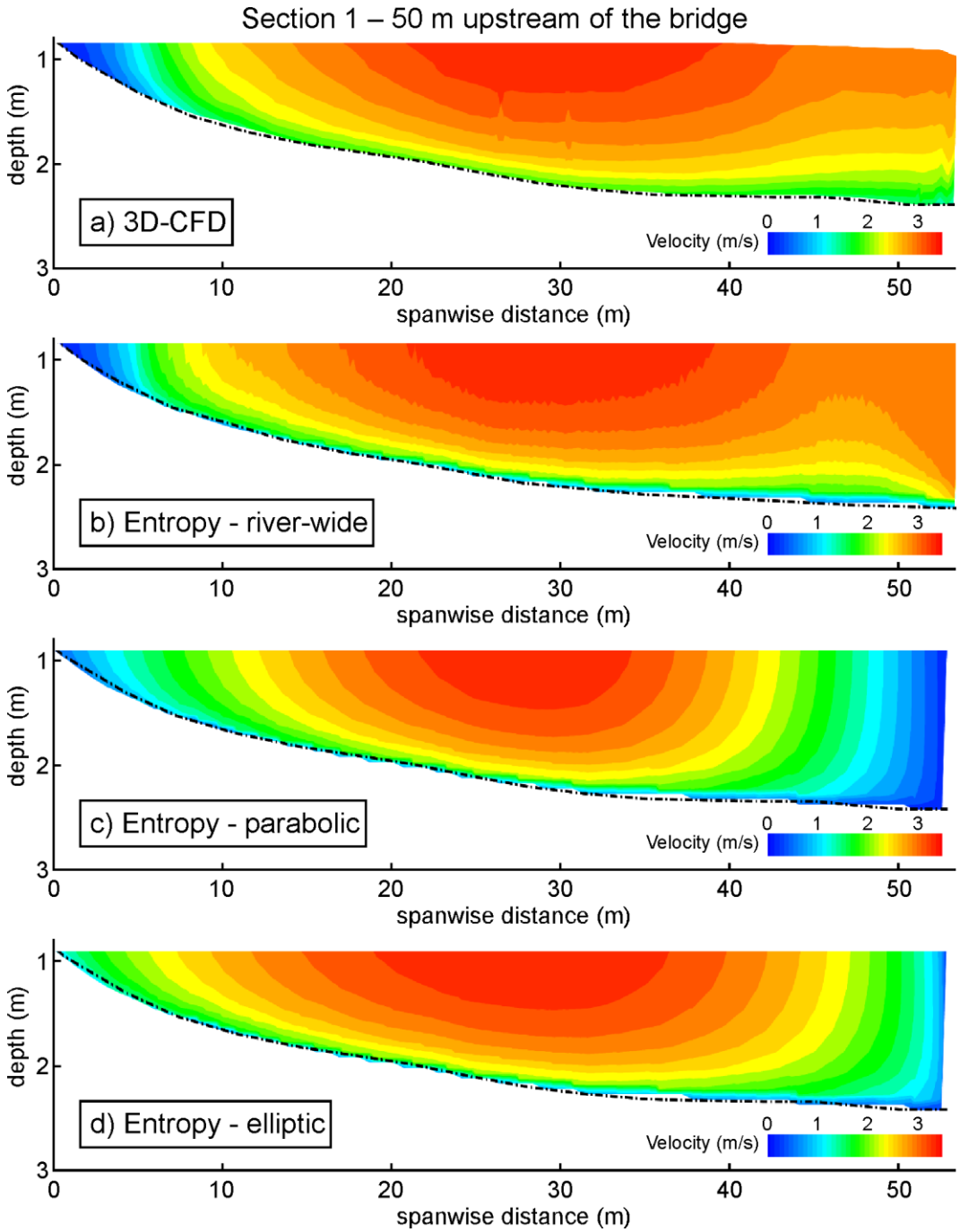

Figure S9. Flood event of 2022, cross-section 1 (50 m upstream of the bridge). Cross-sectional velocity distribution computed with the 3D-CFD model (a), and the entropy theory forced with (b) the river-wide surface velocity, (c) the parabolic, and (d) and elliptic spanwise velocity distribution.

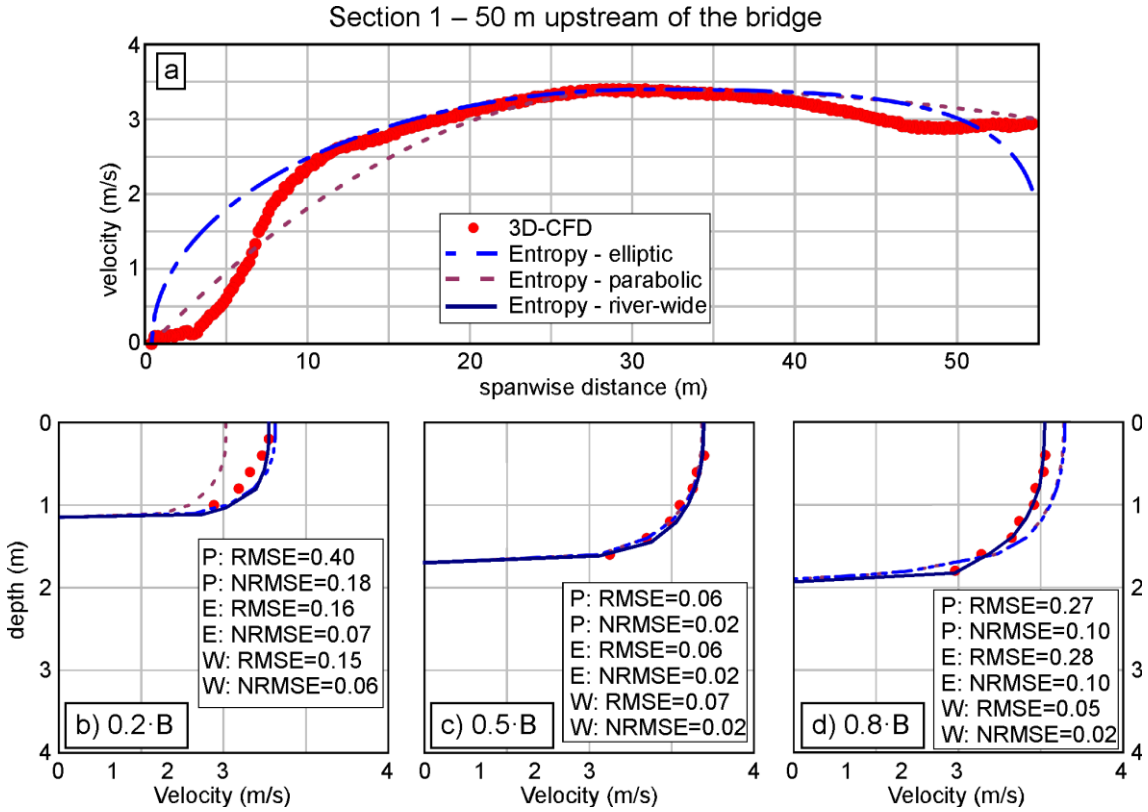

Figure S10. Flood event of 2022, cross-section 1 (50 m upstream of the bridge). Spanwise distribution of the surface velocity (a); comparison of vertical distributions of velocity at 0.2*B* (b), 0.5*B* (c), and 0.8*B* (d).

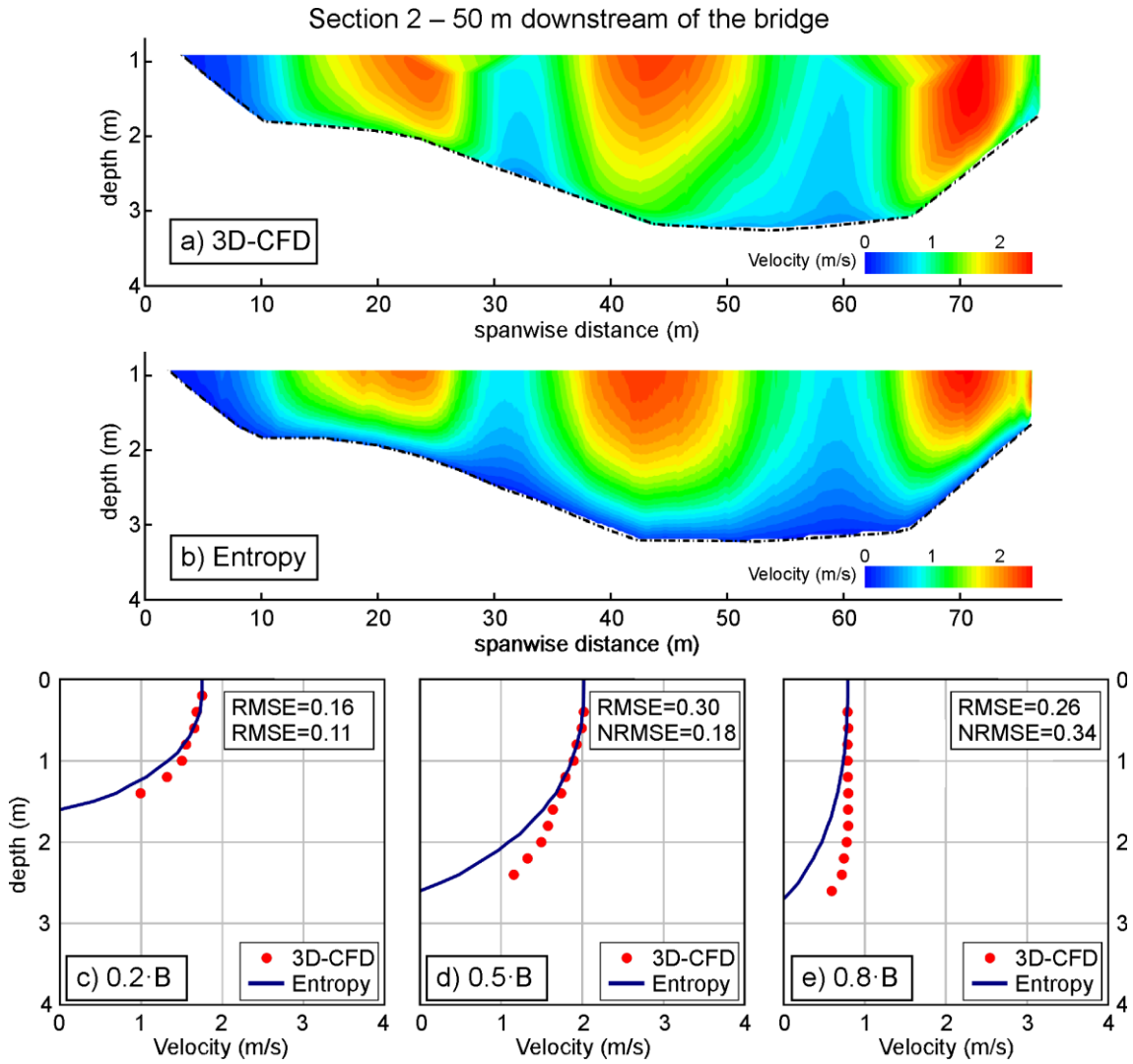

Figure S11. Flood event of 2022, cross-section 2 (50 m downstream of the bridge). Velocity distributions provided by (a) the 3D-CFD model, and (b) the entropy model forced with the river-wide distribution of the free-surface velocity. Comparison of vertical distributions of velocity at 0.2*B* (c), 0.5*B* (d), and 0.8*B* (e), where *B* is the width of the cross-section.

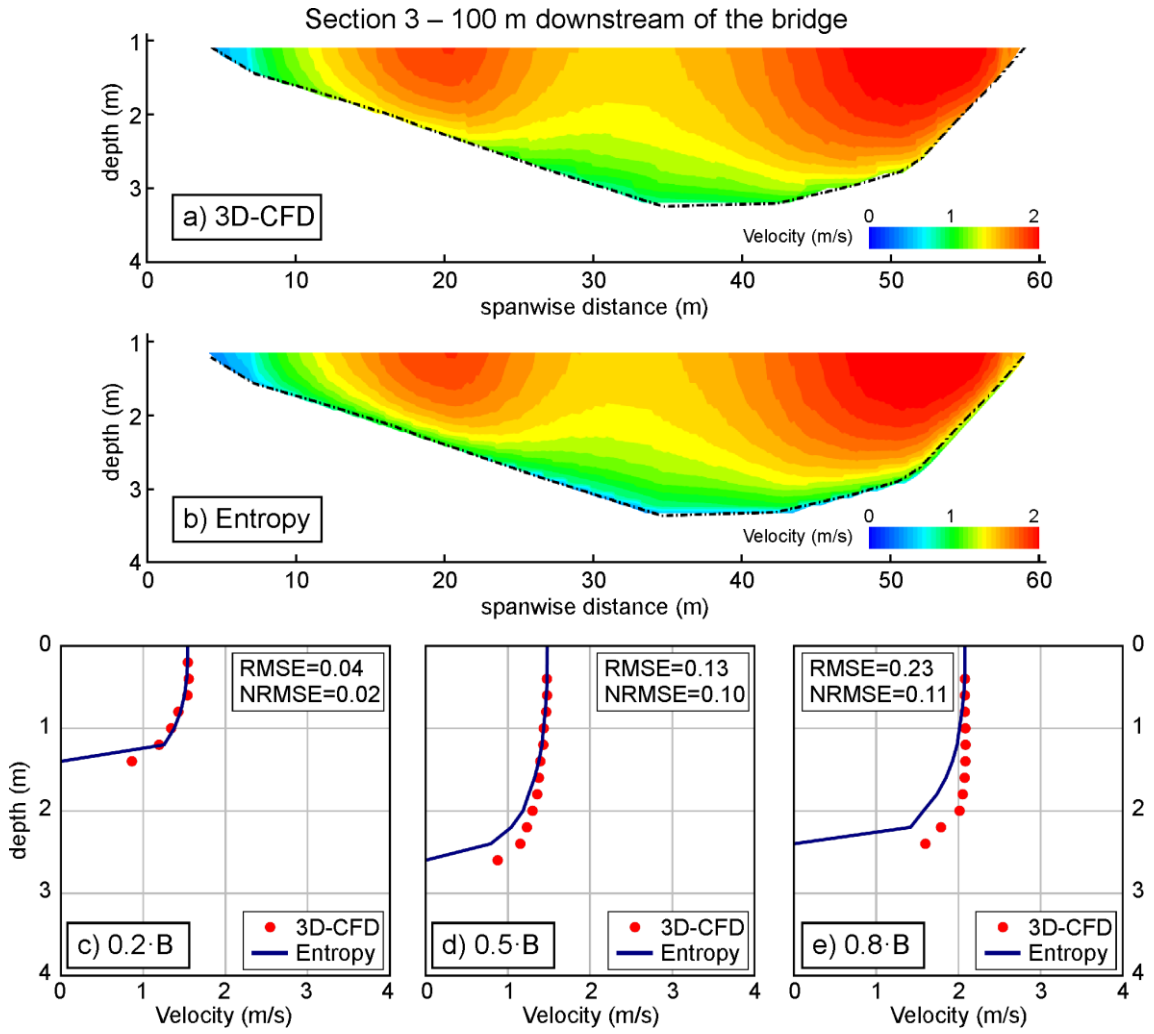

Figure S12. Flood event of 2022, cross-section 3 (100 m downstream of the bridge). Velocity distributions provided by (a) the 3D-CFD model, and (b) the entropy model forced with the river-wide distribution of the free-surface velocity. Comparison of vertical distributions of velocity at 0.2*B* (c), 0.5*B* (d), and 0.8*B* (e), where *B* is the width of the cross-section.

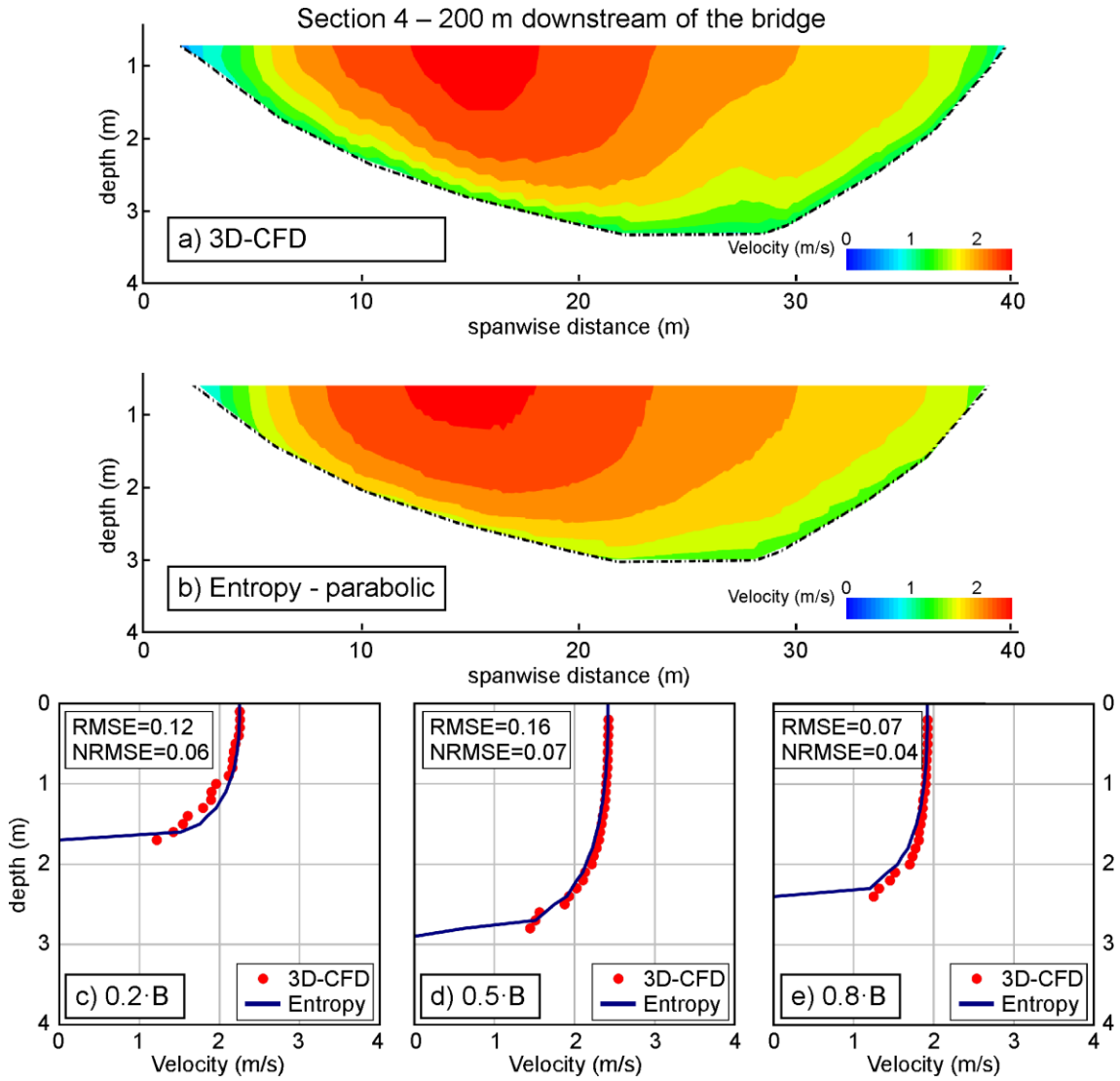

Figure S13. Flood event of 2022, cross-section 4 (200 m downstream of the bridge). Velocity distributions provided by (a) the 3D-CFD model, and (b) the entropy model forced with the river-wide distribution of the free-surface velocity. Comparison of vertical distributions of velocity at 0.2*B* (c), 0.5*B* (d), and 0.8*B* (e), where *B* is the width of the cross-section.

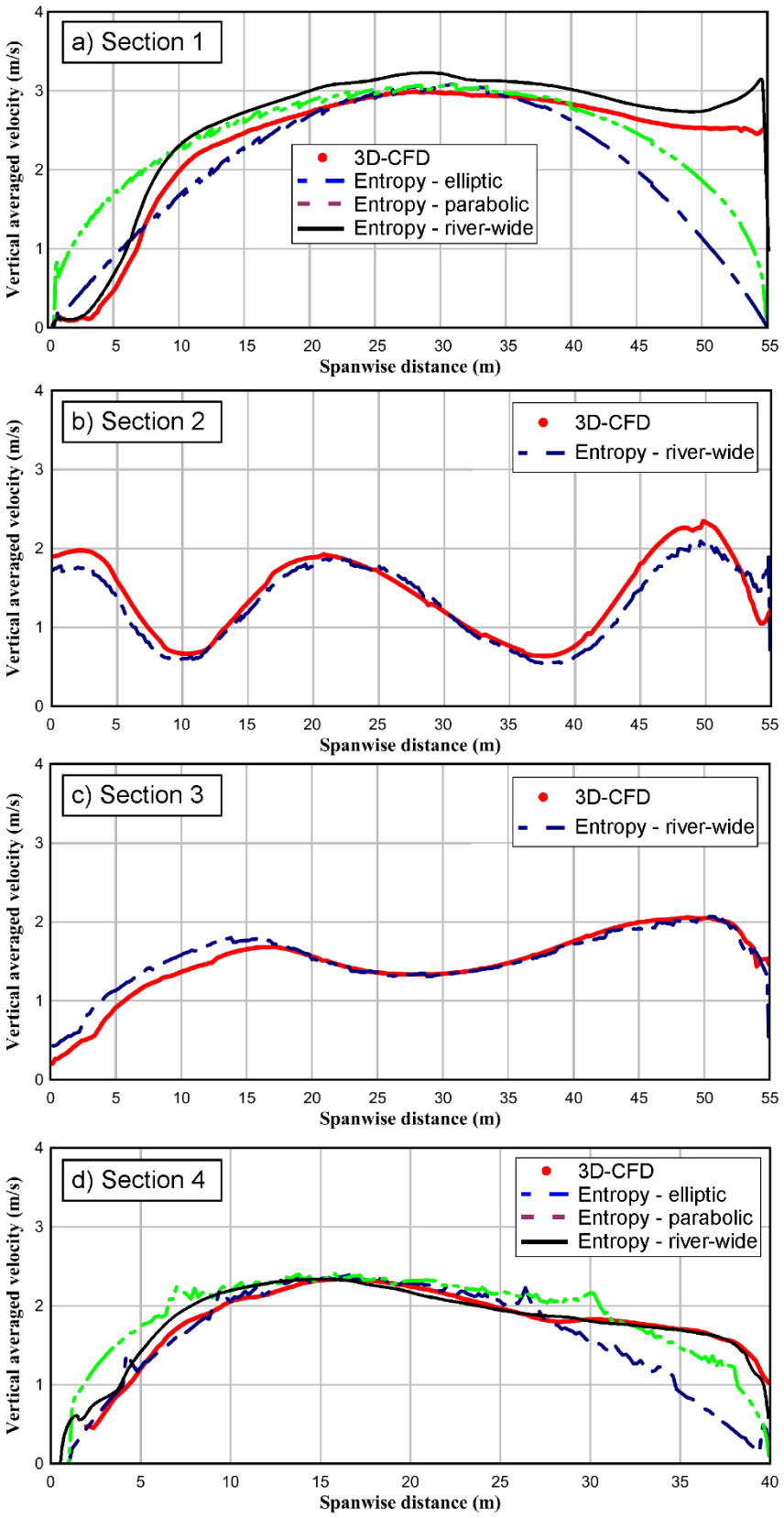

Figure S14. Flood event of 2019. Depth-averaged spanwise velocity distribution at the four cross-sections.